The Astrophysical Journal, 614:979–989, 2004 October 20

TESTING BLEND SCENARIOS FOR EXTRASOLAR TRANSITING PLANET CANDIDATES. I. OGLE-TR-33: A FALSE POSITIVE

Guillermo Torres,[1] Maciej Konacki,[2] Dimitar D. Sasselov,[1] and Saurabh Jha[3]

Received 2004 April 23; accepted 2004 June 25

ABSTRACT

We report high-resolution spectroscopic follow-up observations of the faint transiting planet candidate OGLE-TR-33 ($V = 14.7$), located in the direction of the Galactic center. Small changes in the radial velocity of the star were detected that initially suggested the presence of a large planet or brown dwarf in orbit. However, further analysis revealed spectral line asymmetries that change in phase with the 1.95 day period, casting doubt on those measurements. These asymmetries make it more likely that the transit-like events in the light curve are the result of contamination from the light of an eclipsing binary along the same line of sight (referred to as a "blend"). We performed detailed simulations in which we generated synthetic light curves resulting from such blend scenarios and fitted them to the measured light curve. Guided by these fits and the inferred properties of the stars, we uncovered a second set of lines in our spectra that correspond to the primary of the eclipsing binary and explain the asymmetries. Using all the constraints from spectroscopy, we were then able to construct a model that satisfies all the observations and to characterize the three stars based on model isochrones. OGLE-TR-33 is fully consistent with being a hierarchical triple system composed of a slightly evolved F6 star (the brighter object) near the end of its main-sequence phase and an eclipsing binary with a K7–M0 star orbiting an F4 star. The application to OGLE-TR-33 of the formalism developed to fit light curves of transit candidates illustrates the power of such simulations for predicting additional properties of the blend and for guiding further observations that may serve to confirm that scenario, thereby ruling out a planet. Tests such as this can be very important for validating faint candidates.

Subject headings: binaries: eclipsing — line: profiles — planetary systems — stars: evolution — stars: individual (OGLE-TR-33)

1. INTRODUCTION

Precise radial velocity searches around nearby, relatively bright stars have yielded more than 100 extrasolar planet detections to date, with orbital periods ranging from 2.5 days to nearly 15 yr (Schneider 2004). The discovery of transits in the case of HD 209458b (Henry et al. 2000; Charbonneau et al. 2000) made it possible for the first time to measure the radius of the planet, as well as the inclination angle which removes the spectroscopic $\sin i$ ambiguity in the mass. This opened a new era in the study of these objects, allowing astronomers to probe the structure and evolution of extrasolar giant planets and leading even to the first detection of a planetary atmosphere outside the solar system (Charbonneau et al. 2002; Vidal-Madjar et al. 2003, 2004).

With the realization that a fair number of the planets found by the Doppler technique have relatively short orbital periods (a few days), which makes the detection of transits across the disk of the parent star much more likely, photometric searches for such events have become a potentially important discovery tool. Numerous searches are underway (and others have already been completed) that target a variety of stellar populations, including globular clusters, open clusters, and the general field (see Horne 2003). The search strategies of these programs are quite varied (field of view and density of stars, magnitude limit, cadence of observations, passbands, etc.), but they all aim at millimagnitude photometric precision and frequent observations to detect small drops in brightness of a few percent with a typical duration of only a few hours.

One of these searches, the Optical Gravitational Lensing Experiment (OGLE; Udalski et al. 1992), was not originally designed to search for planets but in its latest incarnation (OGLE-III) has turned out to be one of the most successful in finding transit candidates. A total of 64 candidates have been reported by Udalski et al. (2002c, 2002b, 2003) in three fields in the direction of the Galactic center. In many cases, the candidates display light curves strongly resembling that of HD 209458. A further 73 transit candidates were reported in three other fields in the constellation of Carina (Udalski et al. 2002a, 2003). Dozens of other candidates have been found by other teams, although only a fraction of them have actually been reported in the literature.

In general, photometry alone cannot unambiguously establish whether the object responsible for the transit is a planet (less than $\sim 13 M_J$), a brown dwarf ($\sim 13 M_J$–$80 M_J$), or a more massive stellar companion. The problem is compounded by the fact that the radius is nearly constant for objects with masses between 0.001 and 0.1 $M_\odot$ (see, e.g., Oppenheimer et al. 2000). Furthermore, light curves showing transit-like events of depth similar to that produced by, e.g., a Jupiter-sized planet around a solar-type star ($\sim$1%) can also be produced by other astrophysical phenomena. These include grazing geometry in a regular eclipsing binary, blending of the light of an eclipsing binary with a single star that may or may not be physically associated (and that dilutes the transit depth), or an eclipse produced by a small stellar companion passing in front of a large (early-type or giant) primary star. Therefore, careful follow-up of these candidates becomes crucial to establish their true nature, especially given that the frequency of these "false

[1] Harvard-Smithsonian Center for Astrophysics, 60 Garden Street, Cambridge, MA 02138; gtorres@cfa.harvard.edu.
[2] California Institute of Technology, Division of Geological and Planetary Sciences, MS 150-21, Pasadena, CA 91125.
[3] Department of Astronomy, University of California, Berkeley, CA 94720.

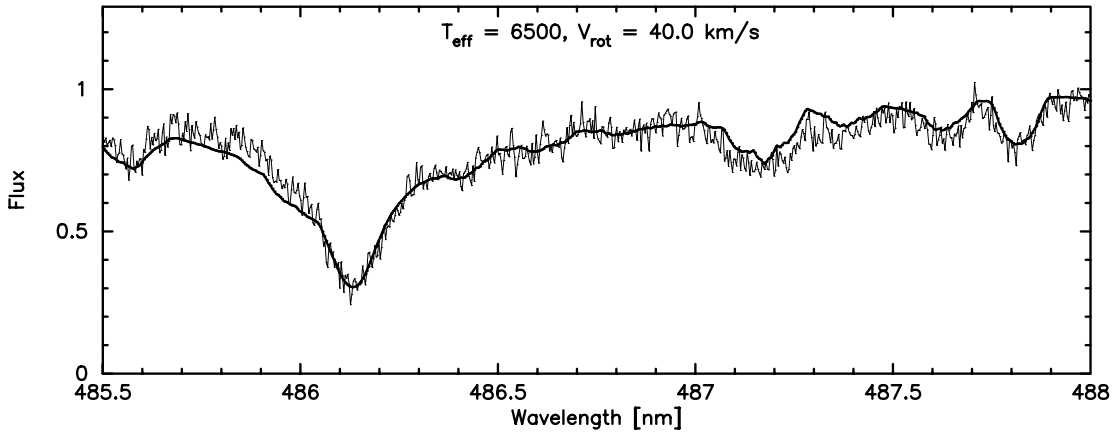

FIG. 1.—Observed spectrum of OGLE-TR-33 (obtained by co-adding the four individual spectra) compared to our best-fit theoretical spectrum (smooth line), used to derive the stellar properties (see text).

positive'' detections appears to be very high (see, e.g., Latham 2003; Konacki et al. 2003a; Brown 2003).

In this paper we focus on the transit candidate OGLE-TR-33, from the first of the OGLE-III samples toward the bulge of the Galaxy. This same sample led recently to the confirmation of the extrasolar transiting planet around the faint ($V = 16.6$) star OGLE-TR-56 (Konacki et al. 2003a; Torres et al. 2004), only the second case known at the time. OGLE-TR-33 also appeared initially to be among the very best candidates for harboring a planetary companion. It has a photometric period of 1.95 days and a transit depth of 3.4% in the I band as determined by the OGLE team. However, as we describe below, follow-up work shows this *not* to be a transiting planet, but instead a very interesting example of a blend configuration with an eclipsing binary in a hierarchical triple system. We use this case to illustrate the importance of examining the spectral line profiles for variable asymmetries, and we develop a technique to model the light curve in detail in order to test various blend scenarios that satisfy all observational constraints. Such models allow one to accurately characterize the properties of the contaminating eclipsing binary and to predict other observable quantities. Techniques such as this are valuable aids for validating transit candidates, particularly faint ones, which are rapidly increasing in number as photometric surveys continue operation.

2. SPECTROSCOPIC OBSERVATIONS

OGLE-TR-33 ($17^{\rm h}56^{\rm m}41\overset{\rm s}{.}19$, $-29^\circ40'05\overset{''}{.}3$: J2000.0) was originally selected as a good candidate after careful low-resolution spectroscopic reconnaissance of the entire OGLE-III bulge sample carried out in 2002 (Konacki et al. 2003b). That work was designed to reject cases with obvious stellar companions on the basis of their large radial velocity variations (tens of km s^{-1}) or early spectral type. Only six of the 39 candidates in the sample subjected to this filtering survived, and these were then observed at much higher spectral resolution to try to detect low-amplitude velocity variations presumably indicative of a companion of planetary mass. The high-resolution observations of OGLE-TR-33 discussed in this paper were conducted with the Keck I telescope using the HIRES instrument (Vogt et al. 1994) on 2002 July 24–27. We obtained one spectrum on each of four nights, with an exposure time of 30 minutes resulting in signal-to-noise ratios of 15–20 pixel^{-1}. The wavelength coverage (36 echelle orders) is approximately 385–620 nm at a resolving power of $\lambda/\Delta\lambda \sim 65,000$. The usual strategy for Doppler planet searches with this instrument is to use the iodine gas absorption cell as the wavelength fiducial, which makes it possible to achieve meter per second accuracy in the radial velocities for bright stars (e.g., Butler et al. 2003). Because of the faintness of our target ($V = 14.7$), however, the decision was made not to use the iodine cell in this case in order to minimize light loss, essentially trading off precision for increased signal. For the wavelength calibration, we relied on exposures of a thorium-argon lamp taken before and after each stellar exposure. The limit to the velocity accuracy attainable with this procedure is ultimately set by the stability of the spectrograph (see below). The echelle reductions were performed using the MAKEE package (Barlow 2002), including scattered light correction and cosmic-ray removal. Orders blueward of ~400 nm were not used because of low signal.

Radial velocities were obtained by cross-correlation using the *xcsao* task (Kurtz & Mink 1998) running under IRAF.[4] The template used is a synthetic spectrum chosen to closely match the star (which was assumed to be of solar metallicity) and also broadened to match the resolution of the instrument. The main parameters of this template (effective temperature, $T_{\rm eff}$, and surface gravity, $\log g$) were estimated by comparison with a high signal-to-noise ratio spectrum made by co-adding our four spectra. The model atmospheres are based on ATLAS9, along with opacities and extensive line lists developed by Kurucz (1993). We have added tools to compute the radial-tangential macroturbulent velocity field broadening, as well as complex rotational broadening of spectral lines. The code has been found to perform very well for solar-type stars (spectral type F–K). We fitted a large number of metal absorption lines of different ionization and excitation stages, as well as the core and wings of the Balmer Hβ line. The parameters we derive correspond to a mid-F star with $T_{\rm eff} \approx 6500$ K and a rotational broadening $v \sin i$ of ~40 km s^{-1}, quite typical of F stars in the field. The constraint on the surface gravity is weaker, but we estimate that it is not lower than $\log g = 3.5$. Figure 1 shows our fit to the observed spectrum in the region of the Hβ line.

Our radial velocities for OGLE-TR-33 are the weighted average of the 31 orders we used and have typical uncertainties of ~0.5 km s^{-1}, except for the weaker exposure on the first night. This is much larger than we obtained for other OGLE

[4] IRAF is distributed by the National Optical Astronomy Observatories, which is operated by the Association of Universities for Research in Astronomy, Inc., under contract with the National Science Foundation.

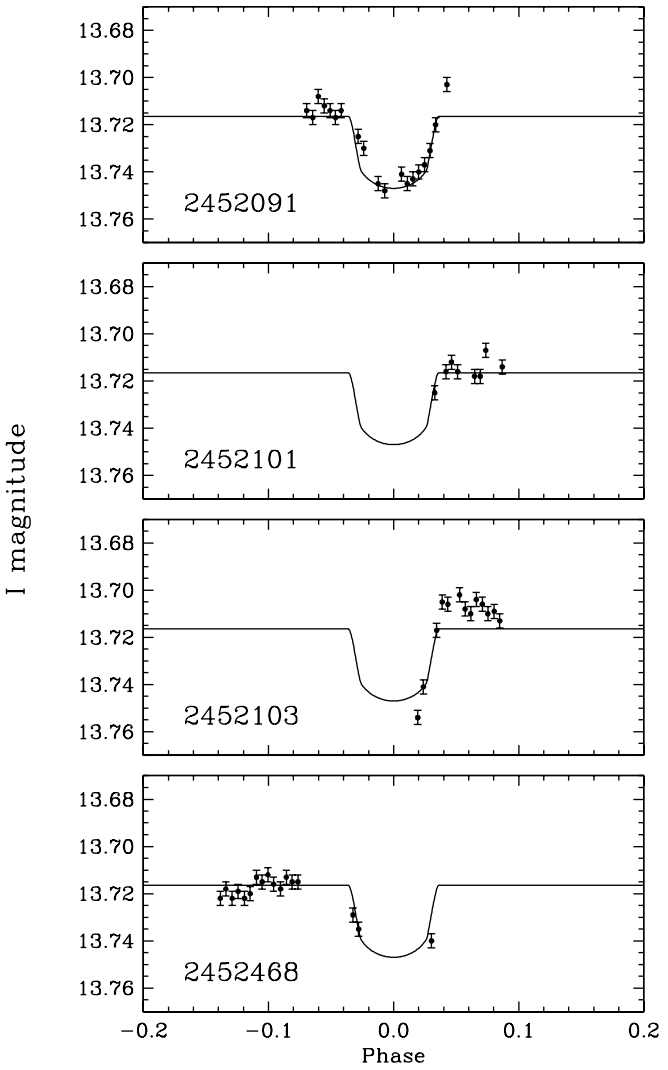

FIG. 2.—Individual transits recorded by the OGLE team for OGLE-TR-33. Julian dates for the corresponding night are indicated in each panel. The solid line drawn for reference is a transit model described in § 4 (see also Fig. 3).

targets during the same run ($\sim$100 m s^{-1}; Konacki et al. 2003b), which is due to the large rotational velocity of the star.

Two stars with known planets were observed each night as velocity standards: HD 209458 and HD 179949. Because their spectroscopic orbits are known (Mazeh et al. 2000; Naef et al. 2004; Tinney et al. 2001), we used them to evaluate the stability of the instrument over the four nights of our run. Suitable templates based on the same models as above were computed using the stellar parameters reported for these stars in the literature. Velocity reductions of HD 209458 and HD 179949 with the standard Th-Ar technique indicate that instrumental shifts are at the level of 100 m s^{-1} or less (see Konacki et al. 2003a, 2003b).

3. PHOTOMETRIC DATA

OGLE-TR-33 was monitored photometrically by the OGLE group during the 2001 and 2002 seasons. A total of 396 observations were collected by that team in the I band,[5] with a nominal precision of 0.003 mag. In what follows, however, we have chosen to adopt a more realistic value for the error of 0.006 mag, based on the scatter outside of eclipse. Four transit-like events have been recorded (see Fig. 2), although only one is reasonably complete. The transit ephemeris that has been derived from them,[6] and which we adopt in the following, is

$$T(\mathrm{HJD}) = 2,452,062.49338 + 1.95320E, \qquad (1)$$

where E is the number of cycles elapsed since the reference epoch. The depth of the transit as reported by the OGLE team is 3.4% and the mean brightness of the system is $I = 13.71$, with an estimated color index of $V - I = 0.95$ (Udalski et al. 2002c).

The light curve of OGLE-TR-33 was examined independently by Drake (2003) and Sirko & Paczyński (2003) for signs of variability outside of eclipse (reflection effects, gravity brightening, and ellipsoidal variability), which would almost certainly indicate a stellar companion as opposed to a planetary-mass object. Neither study found any significant variations. Further information on the nature of the companion can be gleaned from the shape and duration of the transits themselves, as shown by Seager & Mallén-Ornelas (2003), which allow the properties of the primary star to be inferred directly. In principle, this can be used to rule out planetary companions in some cases, e.g., if the stellar properties are inconsistent with those of normal stars or with other information such as the spectral type. In practice, the usefulness of the test depends strongly on the precision and phase coverage of the photometry, and unfortunately for OGLE-TR-33 the ingress and the bottom of the transit are not very well covered. While the resulting parameters for the star appear roughly consistent with those of a main-sequence object and would not seem to clearly rule out a planetary companion, we consider these results to be inconclusive in this case.[7]

4. SPECTROSCOPIC RESULTS

Significant changes are evident in our Keck radial velocities for OGLE-TR-33 over four consecutive nights, with a peak-to-peak variation of nearly 4 km s^{-1}. As can be seen using eq. (1), the observations were all taken near the quadratures, where the velocity excursion is expected to be the largest. In Figure 3*a* we show those observations folded with the known ephemeris. A Keplerian orbital fit is also shown for an assumed circular orbit as expected on theoretical grounds given the relatively short period. Since the period and epoch are known sufficiently well from the photometry, the only two remaining adjustable

[5] Results from and more information on the OGLE experiment are available at http://bulge.princeton.edu/~ogle.

[6] Results from the OGLE-III search for planetary and low-luminosity object transits are available at http://bulge.princeton.edu/~ogle/ogle3/transits/transits.html.

[7] Seager & Mallén-Ornelas (2003) have shown that the stellar mass, radius, and density can be estimated readily by careful measurement of the depth of the transit (relative change in flux, ΔF), its total duration (t_T), and the duration of the flat portion (t_F), along with the knowledge of the orbital period. For OGLE-TR-33, we measure those parameters to be $\Delta F = 0.034$, $t_T = 0.074$, and $t_F = 0.050$ (the latter two in phase units), although with large uncertainties due to incompleteness of the light curve. The resulting stellar mass (1.74 $M_\odot$), radius (1.56 $R_\odot$), and density [$\log(\rho/\rho_\odot) = -0.34$] are roughly consistent with those of an F0 main-sequence star (e.g., Cox 2000), allowing in principle for the possibility that the companion is indeed a planet. There may be a slight inconsistency, however, between that spectral type and the effective temperature for the star we estimated above (6500 K), and in addition the inferred size of the companion is perhaps somewhat large for a planet (0.29 $R_\odot$, or 2.8R_J). In view of the difficulty in estimating the light-curve parameters, and the fact that the measured values are close to the limit of validity of the equations of Seager & Mallén-Ornelas (2003), we prefer to regard the above results as inconclusive.

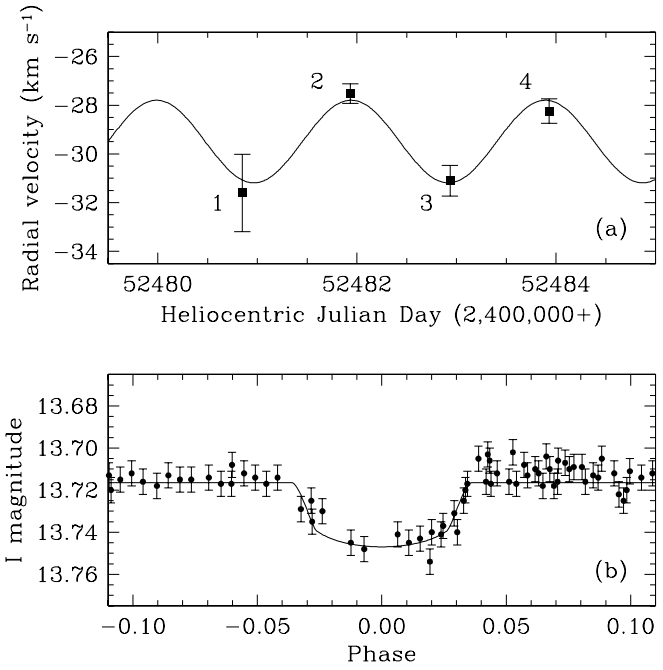

FIG. 3.—(*a*) Keplerian orbital fit to the formal radial velocities of OGLE-TR-33. The phasing of the curve is fixed from eq. (1), and only the velocity amplitude and an offset have been adjusted. Observations are numbered to facilitate the referencing with Fig. 4. (*b*) Transit light curve of OGLE-TR-33, and our fit assuming the companion is a planet (see text).

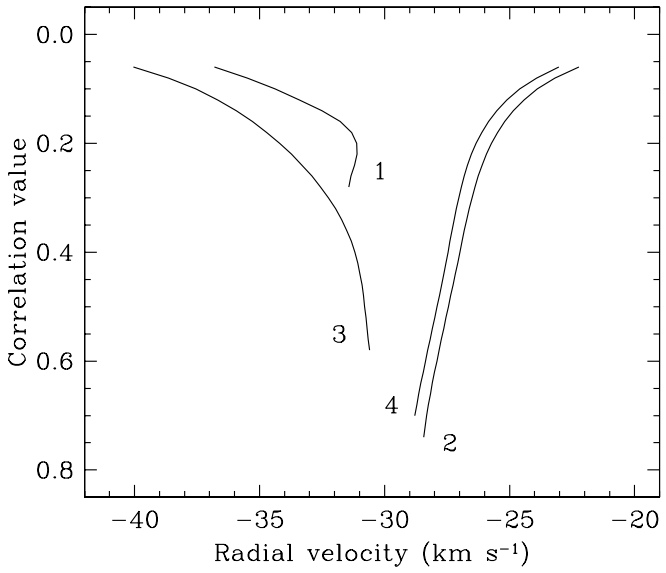

FIG. 4.—Spectral line bisectors for OGLE-TR-33 computed from the correlation function, which represents the average spectral line. The core of the line is toward the bottom. The profiles for each date are labeled as in Fig. 3*a*. The asymmetries are obvious, and their change in step with the phase is not normally expected from orbital motion.

parameters are the velocity amplitude, K, and the center-of-mass velocity, γ. For these we obtained $K = 1.70 \pm 0.27$ km s^{-1} and $\gamma = -29.49 \pm 0.27$ km s^{-1}. The amplitude is highly significant compared to its error. For an edge-on configuration such as this would appear to be, the formal mass we infer for the orbiting companion is $12.6 M_J \pm 1.7 M_J$, implying that it is a large planet or perhaps a brown dwarf.

With the parameters adopted for the primary star in § 2, a typical radius for an F star of 1.4 $R_\odot$, and an appropriate linear limb-darkening coefficient in the I band of $u_I = 0.51$ (Claret 2000), we fit the transit light curve using the formalism of Mandel & Agol (2002). The solution is shown in Figure 3*b* along with the OGLE photometry. The inclination angle derived is essentially 90°, and the inferred radius of the companion is $2.1 R_J \pm 0.1 R_J$.

However, further investigation revealed spectroscopic evidence that casts serious doubt on the interpretation that the velocities we measured are the result of the orbital motion of a planet or a brown dwarf. We noticed, for instance, that the velocities were quite sensitive to some of the details of how they were computed with *xcsao*. Specifically, they changed systematically and significantly as a function of the fraction of the cross-correlation peak considered in computing its centroid.[8] The velocity variations (semiamplitude K) seemed to increase as we included portions of the correlation peak farther out on the wings, which is a rather strong indication that the correlation peak (and therefore the mean line profile) is asymmetric. Furthermore, the asymmetry appeared to change sides in phase with the velocities. Such behavior is not expected from the simple Keplerian motion of the star in its orbit. Similar disproving evidence has recently been found in at least two other cases that appeared initially to be substellar companions as well (Queloz et al. 2001; Santos et al. 2002).

In order to examine the line asymmetries in OGLE-TR-33 more closely, we computed the line bisectors (see, e.g., Gray 1992) determined directly from the correlation function, which is representative of the average shape of a spectral line for the star. The individual correlation functions for each echelle order were added together, resulting in an average line profile with much higher signal. The line bisectors for each of our four nights are shown in Figure 4 on an absolute velocity scale, and with the core of the line toward the bottom. In addition to the shifts, the asymmetries (curved bisectors) are obvious and are quite large, spanning several km s^{-1}. For comparison, the line bisectors in the Sun and similar stars (which display the well-known C shape because of granulation) span only a few hundred m s^{-1}. More importantly, the asymmetries in OGLE-TR-33 are seen to correlate with the phase in the orbit (see Fig. 3*a*), an effect that cannot normally be produced solely by the orbital motion of the star.

The most obvious explanation for the changing asymmetry is the presence of another star in the system, whose spectral lines shift back and forth with the photometric period and distort those of the primary. Note that additional information is given by the type of asymmetry observed. In this case, it is "leading" asymmetry (broader wing of the line profile toward more positive velocities when the measured velocity is also positive compared to γ, and conversely on the other side of the orbit) as opposed to "trailing" asymmetry (see also Sabbey et al. 1995). The latter case would result, for example, from blending of the F star with another star having a constant velocity near γ. This can be ruled out in this case, and therefore the contamination must be from an eclipsing binary, composed perhaps of a late F or early G star (causing the line asymmetries) and an M star. The systemic velocity of this binary must be quite similar to that of the F star. The binary would be

[8] The standard procedure followed in *xcsao* and other similar programs for computing the radial velocity is to fit a parabola to the top portion of the cross-correlation peak, above a certain fraction pkfrac of the maximum, and to use that fit to compute the centroid. The parameter pkfrac can be changed by the user, but defaults to 0.5.

responsible for the transit-like events in the light curve, with the original depth of the eclipses being diluted by the light of the main F star. We examine this hypothesis in more detail below.

5. TESTING THE BLEND MODEL

A fair number of the light curves for extrasolar transiting planet candidates found in various surveys have been explained before as being the result of grazing eclipses, transits by a small star in front of a large star, or blends with an eclipsing binary. Unfortunately, these situations appear to be far more common than anticipated, and more common also than bona fide transiting planets, a fact that is just now beginning to be fully appreciated and that is likely to affect design strategies for future transit searches (see Brown 2003), even those from space. Nevertheless, relatively few blend cases have been documented in detail in the literature (see Mallén-Ornelas et al. 2003; Yee et al. 2003; Latham 2003; Charbonneau et al. 2004). In OGLE-TR-33 there is rather strong evidence that contamination may be the case as well, but we wish to go beyond qualitative explanations and test this hypothesis in a more quantitative way. Our motivation for doing this is to develop general procedures that may serve to test other cases where the evidence for a blend is more subtle or not obvious at all. Such candidates are bound to present themselves in current or future searches and are the most challenging to rule out. The shape and duration of the observed transits provide important constraints on possible configurations involving a contaminating eclipsing binary. Therefore, we first investigate whether the OGLE-TR-33 photometry is consistent with this explanation by simulating realistic binary light curves, including dilution effects. Next we examine our spectra further for direct evidence of lines of another star, guided by the results of the simulations.

5.1. *Simulating Eclipsing Binary Light Curves*

Although the variety of possible eclipsing binaries with which the F star in OGLE-TR-33 could be blended may seem very large, clues from the light curve itself and also from the spectroscopy limit the range considerably. For example, the very short duration of the transits ($\sim$0.07 in phase, or 3.3 hr) indicates that the eclipsing binary is well detached, as opposed to the fairly common W UMa or Algol systems. In addition, there is no evidence of a secondary eclipse, suggesting that the companion is much cooler than the primary. The large asymmetries in the lines of the F star suggest that the primary of the eclipsing binary is shifting back and forth by tens of km s^{-1}, and this would indicate that the companion is a star rather than a substellar object. Therefore, we consider here only detached systems composed of main-sequence stars. In order to generate synthetic light curves to be fitted to the real data, we relied on the computer program EBOP (Popper & Etzel 1981), based on the Nelson-Davis-Etzel model (Nelson & Davis 1972; Etzel 1981), which is adequate for well-detached systems. This model accounts for the oblateness of the stars, as well as the effects of reflection, limb darkening, and gravity brightening. In the following we refer to the primary and secondary of the eclipsing binary as star 1 and star 2, while the F star OGLE-TR-33 itself (which provides "third light" and dilutes the eclipses of the binary) is referred to as star 3. The physical properties of the stars that are needed to generate a light curve are selected from model isochrones, and the two components of the binary are assumed to be on the same isochrone.[9] Whether or not star 3 can be assumed to conform to the same isochrone as the binary will depend on whether the stellar configuration is a physical triple system. If not, the age and even the chemical composition can be different, and a separate isochrone is used (see below).

For each binary component, the selected isochrone provides the radius (R), $\log g$, $T_{\rm eff}$, and absolute magnitudes in the visual band (M_V) and in the I band (M_I). We used these to compute some of the parameters needed to generate a light curve with EBOP, which are J (the central surface brightness of the secondary in units of that of the primary), $r_1 \equiv R_1/a$ (the radius of the primary in units of the semimajor axis, a), $k \equiv r_2/r_1$ (the ratio of the radii), $q \equiv M_2/M_1$ (the mass ratio), and the limb-darkening coefficients in the I band (linear approximation). The latter were interpolated from the tables by Claret (2000) for the $T_{\rm eff}$ and $\log g$ of each component. The gravity brightening coefficients were set to values appropriate for convective stars (0.32). The orbit of the binary was assumed to be circular, and the inclination angle in this particular case can be set to 90° for simplicity and also because the flat-bottomed transits in OGLE-TR-33 suggest total eclipses (although in principle the inclination can be left as an additional free parameter; see below).

The surface brightness ratio J in the I band was derived from the expression

$$J = \frac{1}{k^2}\frac{1-u_1/3}{1-u_2/3}\,10^{-0.4\left(M_{I,2}-M_{I,1}\right)}, \qquad (2)$$

where u_1 and u_2 are the limb-darkening coefficients for the primary and secondary and the last term represents the ratio of the luminosities in the I band in terms of the absolute magnitudes given by the isochrones (see, e.g., Kallrath & Milone 1999).

Dilution of the depth of the binary eclipses by the light from star 3 is controlled by the "third light" parameter, l_3, which is defined in EBOP so that the sum of the three luminosities is unity. Since the absolute magnitude of star 3 is also given by the isochrones for its adopted mass and age, third light (in the I band) was computed simply as

$$l_3 = \left(1 + 10^{-0.4\left(M_{I,1}-M_{I,3}\right)} + 10^{-0.4\left(M_{I,2}-M_{I,3}\right)}\right)^{-1}. \qquad (3)$$

For each trial combination of a primary and secondary for the eclipsing binary and the fixed properties of star 3 (see below), a synthetic light curve can be generated and compared with the observations in a least-squares sense. In practice, we explore a wide range of primary and secondary masses and search for a minimum of the χ^2 sum.

The blend model described above is quite general and allows us to predict a number of properties of the eclipsing binary components that are potentially testable with the observations in hand. Given that the primary is the most likely of the two

[9] The reliability of stellar evolution models and their usefulness for predicting the physical properties of stars is well supported by the strong observational constraints provided by eclipsing binaries, at least in the range from ~1 to 10 $M_\odot$. For low-mass stars of spectral type M, however, all existing evolutionary models become less realistic to some extent because of limitations in the equation of state, convection prescriptions, missing opacities, and/or the boundary conditions adopted. We discuss these limitations and their impact on the present analysis below.

stars in the eclipsing binary to be detectable spectroscopically, one of the quantities of interest is the velocity amplitude in its orbit, in kilometers per second,

$$K_1 = 212.91 \times P^{-1/3} \frac{M_2}{(M_1 + M_2)^{2/3}}, \quad (4)$$

which follows directly from the masses indicated by the isochrone (in units of the solar mass) and the known period P in days.

Under the assumption that star 1 is rotating synchronously with the orbital motion (a reasonable assumption given that the period is short; see Hut 1981), the projected rotational velocity in terms of the radius from the isochrone (expressed in units of $R_\odot$) is given, in kilometers per second, by

$$v_1 \sin i = \frac{50.61}{P} R_1 \sin i. \quad (5)$$

The relevance of this quantity here is that it can affect the broadening of the spectral lines of star 1 and can make it more difficult to detect, particularly if it is faint. Although strictly speaking the inclination angle in equation (5) is that of the spin axis, it can be safely assumed to be the same as that of the orbit, or close to 90° for all practical purposes (Hut 1981).

Since the brightness of each star can also be predicted from the isochrone, the light ratio between star 1 and star 3 (which is in principle directly observable) is simply

$$L_1/L_3 = 10^{-0.4(M_{V,1} - M_{V,3})}. \quad (6)$$

We have expressed it here in the visual band rather than in the I band because the observational constraint we have on this ratio comes from our optical spectra, which are best matched to the V band.

Given that a large fraction of all field stars are in multiple systems (e.g., Duquennoy & Mayor 1991; Tokovinin 1997; Tokovinin & Smekhov 2002), it may be expected that in many cases the blend configuration will correspond to a physical triple system. In other blend situations, the eclipsing binary could be in the background or foreground. For convenience in such cases we parameterize the relative distance between the binary and the third star in terms of the difference in the distance moduli, ΔM, so that $d_{\rm bin} = d \times 10^{0.2\Delta M}$ (where d is the distance to star 3). The different distances for the binary and star 3 introduce the need to account for differential extinction, which can have a significant effect. For a given combination of three stars, it will change the amount of third light, l_3, and also the predicted light ratio L_1/L_3. Differential extinction (e.g., in magnitudes per kiloparsec) is a strong function of the line of sight, and is essentially an unknown quantity because of the unknown distribution of absorbing material in the Galaxy. A representative value often mentioned in the literature is 1 mag kpc^{-1}. However, the true value is likely to be very different in any direction one may choose, since dust appears to be highly patchy not only across the sky but also in the radial direction (particularly toward the Galactic center, where the OGLE fields are located). Nevertheless, we may adopt the prescription that the total extinction up to a certain distance d (in parsec) is given by $A_V = a_V(d/1000)$, where a_V is the coefficient of differential extinction in the visual band (in magnitudes per kiloparsec). We also assume for simplicity that a_V is the same for the eclipsing binary as for star 3. Extinction therefore adds two new unknowns to the problem: the distance d to star 3, and the coefficient a_V. The distance to the binary follows from the value of ΔM.

In order to solve for the new unknowns, we make use of the constraint provided by the total apparent magnitude of OGLE-TR-33 (comprising three stars) in the visual and also in the I band: $I = 13.71$ and $V = 14.66$ (the latter is derived from the $V - I$ color in § 3). We require that the brightness of the three stars (decreased by distance from the observer and by extinction) add up to the measured values in both passbands, thus accounting for differential reddening. The combined light in the visual band is

$$V = V_3 - 2.5 \log\left(1 + 10^{-0.4(V_1 - V_3)} + 10^{-0.4(V_2 - V_3)}\right), \quad (7)$$

where the apparent magnitudes of the three stars are

$$V_1 = M_{V,1} - 5 + 5 \log d + \Delta M + a_V(d/1000)10^{0.2\Delta M}, \quad (8a)$$

$$V_2 = M_{V,2} - 5 + 5 \log d + \Delta M + a_V(d/1000)10^{0.2\Delta M}, \quad (8b)$$

$$V_3 = M_{V,3} - 5 + 5 \log d + a_V(d/1000). \quad (8c)$$

Similar expressions hold for the total magnitude in the I band, with a differential extinction coefficient a_I. For a_I, we adopt the relation given by Cardelli et al. (1989), $a_I = 0.48 a_V$ (assuming $R_V = 3.1$).[10] To account for the effect of extinction in the contribution from third light l_3 and in the predicted light ratio L_1/L_3, the absolute magnitudes in equations (3) and (6) are replaced with the apparent magnitudes given in equations (8a)–(8c) and their analogs for the I band.

To summarize, the parameters to be adjusted in the most general case are the masses M_1, M_2, and M_3, the age of the isochrone(s), i, d, ΔM, and a_V. In practice, the ages and some of the other parameters may be poorly constrained, depending on the quality of the light curve, and may need to be fixed. A value for M_3 can usually be adopted on the basis of the spectral type or estimated effective temperature of the star.

We note finally that once a satisfactory fit to the light curve is achieved, the formalism above makes it straightforward to generate a curve based on the same physical parameters but for a different passband. While the photometric signature from true planetary transits should be independent of wavelength (except for minor effects due to limb darkening; see Tingley 2004), the photometric signature of a blend is in many cases color dependent (but not always; see below), and the predicted depth as a function of wavelength can be tested observationally.

5.2. *Application to OGLE-TR-33*

In our initial simulations for OGLE-TR-33, we assumed that the three stars form a physical triple system. This is based on the similarity between the center-of-mass velocity of the binary and that of the main star, which we infer from the pattern of the spectral line asymmetries (§ 4). An isochrone was selected so as to match our estimates of the properties of star 3, which we assumed to be an unevolved main-sequence star. On the basis

[10] Udalski (2003) has recently reported evidence of anomalous extinction toward the Galactic center, which would imply a somewhat different value for R_V as well as for a_I/a_V. We do not consider these refinements essential here, as they do not significantly change the results.

of its effective temperature, we adopted a mass of 1.3 $M_\odot$ (Cox 2000), solar composition, and a representative age of 2 Gyr. The isochrone was chosen from the series of models by Girardi et al. (2000).[11] Although we obtained a satisfactory fit to the OGLE light curve for a binary consisting of a mid to late F star with $M_1 = 1.25\ M_\odot$ (quite similar to star 3) eclipsed by a late M star ($M_2 = 0.24\ M_\odot$), some of the predicted quantities from equations (4)–(6) conflicted with our spectroscopic observations. In particular, we predicted $L_1/L_3 = 0.81$ in the visual band, implying that we should see a second set of absorption lines in our Keck spectra nearly as strong as those of the main star. While blending and the natural broadening of the lines of the main star ($v \sin i \approx 40$ km s^{-1}) and of star 1 (expected to have a similar rotation) could make this detection slightly more difficult, it would be rather unlikely to be missed, and in addition we would expect to see a flatter-peaked cross-correlation function than we obtain. The evidence described in the next section shows that the spectroscopic light ratio is in fact much smaller ($\lesssim 0.2$), making this scenario untenable. No reasonable change in the age of the isochrone removed this discrepancy.

Relaxing the condition that the three stars are physically associated can also yield good fits to the light curve, for example, if the eclipsing binary is allowed to be in the background so that it is fainter. One such solution is obtained for a binary system ~1 kpc behind star 3, consisting of a mid or late F star ($M_1 = 1.28\ M_\odot$) eclipsed by an M1 star ($M_2 = 0.45\ M_\odot$). The predicted light ratio in this case gives a more acceptable value of $L_1/L_3 = 0.2$. However, the probability of a chance alignment such as this with a binary that happens to have a systemic velocity very close to that of star 3 (as implied by the changing asymmetries noted in § 4) seems rather small.

An alternate way of making the eclipsing binary significantly fainter than star 3, other than placing it in the background, is to make star 3 itself intrinsically *brighter*. The spectroscopic constraints from our Keck spectra only allow us to state that OGLE-TR-33 is not a giant star, but some degree of evolution is allowed by the data as long as the temperature remains close to what we estimate (~6500 K). In particular, if star 3 is beyond the turnoff in the H-R diagram but still on the main sequence, near the end of the hydrogen-burning phase, it can be considerably brighter than an unevolved star with the same temperature. This situation is depicted in Figure 5, where the arrow shows that a difference in brightness of ~2 mag is possible between an evolved and an unevolved F star for an isochrone corresponding to an age of $\log t = 9.05$ (1.12 Gyr) or close to it. The evolved star is of course considerably more massive in this case (1.97 $M_\odot$ instead of 1.3 $M_\odot$, as we had assumed before), but it still has the same effective temperature.

We repeated the fit to the light curve for an evolved star 3 using this isochrone, and we obtained a solution that is marginally better than before but that gives a predicted light ratio in the visual band between star 1 and star 3 that is now much lower: $L_1/L_3 = 0.18$. The χ^2 surface as a function of the mass of star 1 and star 2 has a unique and well-defined minimum (see Fig. 6), and the fit to the photometry is shown in Figure 7. We note that given the quality of the data this solution is just as satisfactory as the transit model fit in Figure 3, although the differences in shape are fairly obvious. The blend model predicts a very shallow secondary eclipse ~0.003 mag deep, but it is undetectable with the present photometry. The resulting masses of the stars comprising the eclipsing binary are $M_1 = 1.39\ M_\odot$ (spectral type approximately F4 V; Cox 2000) and $M_2 = 0.58\ M_\odot$ (K7–M0 V), and their locations on the isochrone are shown in Figure 5. Star 1 is slightly hotter than star 3, but fainter. The predicted velocity semiamplitude and projected rotational velocity of star 1 are $K_1 = 63$ km s^{-1} and $v_1 \sin i = 40$ km s^{-1}. The distance to the triple system is determined to be 3.5 kpc, and the differential extinction coefficient that fits the combined colors is $a_V = 0.23$ mag kpc^{-1}. Tests with a range of inclination angles indicated that the preferred value is in fact 90°. Other parameters of the fit are $r_1 = 0.186$, $k = 0.391$, and $J = 0.121$. Star 3 contributes 85% of the light in the I band.

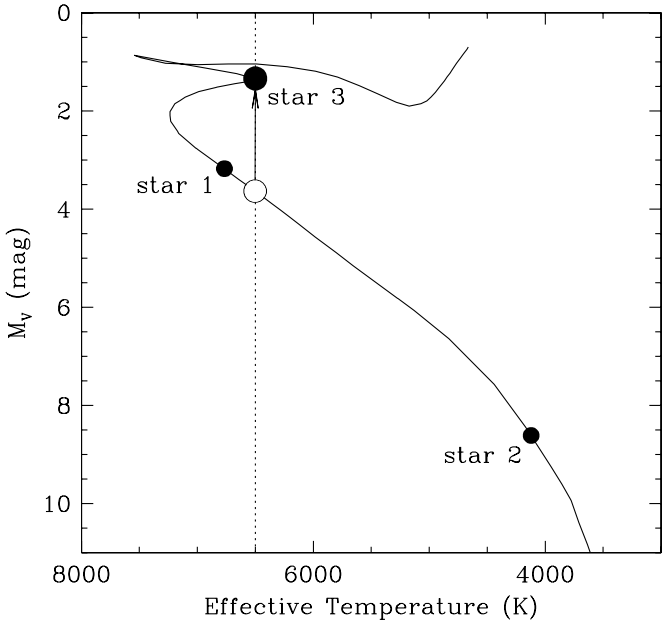

FIG. 5.—Isochrone from Girardi et al. (2000) for an age of 1.12 Gyr and solar composition. The arrow shows that if star 3 is considered to be near the end of its hydrogen-burning phase (at the start of the "blue hook"; *filled circle*), it can be up to 2 mag brighter than a star lower down the main sequence with the same effective temperature (*open circle*). The dotted line represents the 6500 K temperature we determine for OGLE-TR-33. The locations of star 1 and star 2 are the result of a blend model discussed in the text.

The blend model also predicts that the eclipse depth in the V band should be slightly larger than in I but by less than 0.003 mag, a difference that is probably too small to be detected with any confidence in future observations unless the measurement precision is significantly improved. The reason for this is the similarity between the colors of star 1 and star 3, both of which are F stars. Thus, in this particular case the color dependence of the eclipse depth would *not* be a useful diagnostic to rule out a planetary companion.

5.3. *The Lines of Another Star*

The blend scenario in the preceding section has allowed us to make quantitative predictions about the primary of the

[11] Our choice for this application was based on the wide range of ages available and especially the fact that the isochrones reach down to very low masses of 0.15 $M_\odot$, although as indicated in footnote 9 the predicted properties of such low-mass stars are not very realistic. Of particular importance for our purposes is the fact that the predicted radii for such stars have been shown to be underestimated by as much as 10%–20% (Torres & Ribas 2002; Ribas 2003). In order to account for these discrepancies, we have chosen to apply an ad hoc correction to the theoretical radii for low-mass stars by careful comparison of these models with accurate determinations in the eclipsing systems CM Dra, CU Cnc, YY Gem, and V818 Tau (Metcalfe et al. 1996; Torres & Ribas 2002; Ribas 2003). These corrections are typically 1.1–1.2, depending on mass, and they have a modest effect on the depth of the eclipses.

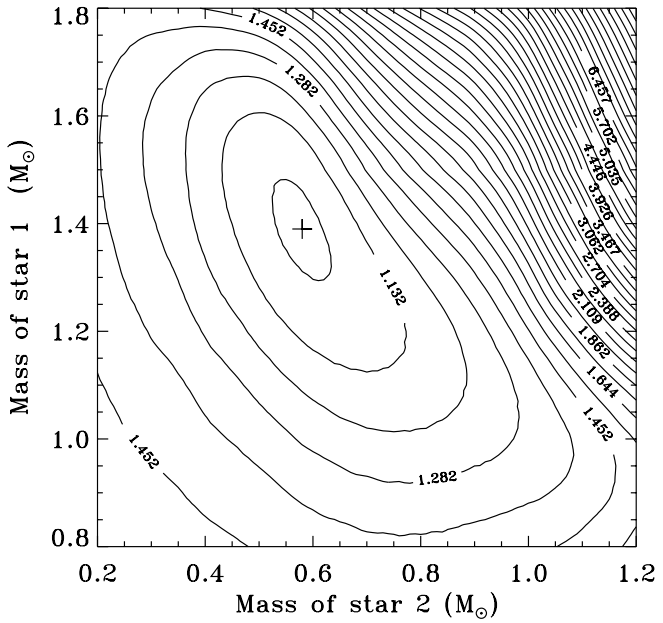

FIG. 6.—Contour plot of the χ^2 surface corresponding to a light curve fit to the photometry for OGLE-TR-33 (star 3). The model has the light of star 3 contaminated by an eclipsing binary assumed to be physically associated (and therefore at the same distance), composed of an F4 main-sequence star and a K7–M0 star. The best-fit masses are indicated by the plus sign (see text). Properties for the three stars are constrained to follow an isochrone with an age of $\log t = 9.05$ (1.12 Gyr), from Girardi et al. (2000). The location of the three stars in the H-R diagram is shown by filled circles in Fig. 5.

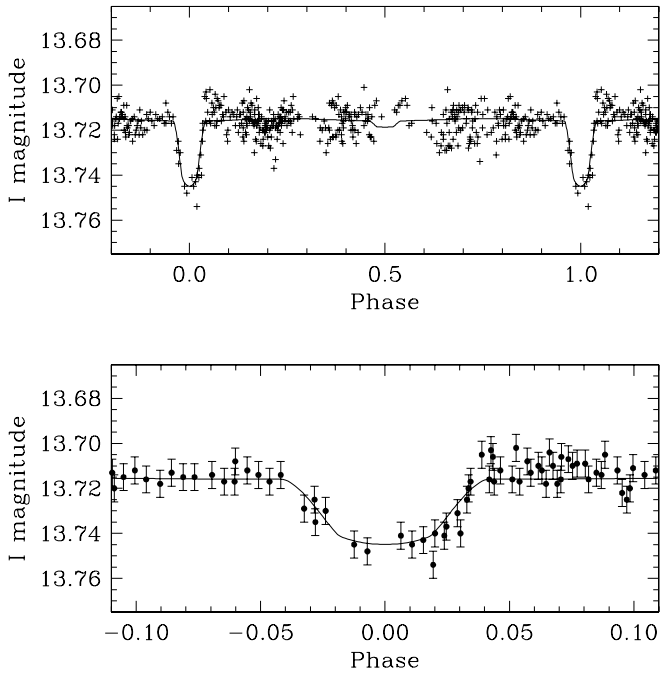

FIG. 7.—Photometry of OGLE-TR-33 together with the light-curve fit resulting from our blend model. In this model the eclipsing binary and the main star are at the same distance (physical triple system), but the main star is near the end of its main-sequence life (see text).

eclipsing binary that can be tested with our data. We expect that if this star is visible in our spectra, it will be roughly 5 times fainter than the main star and its lines will move back and forth with semiamplitude K_1. Although our initial visual inspection of the spectra and cross-correlation functions did not reveal any obvious signs of double lines, in hindsight the asymmetries themselves are a clue to the presence of star 1. Given that the lines of the main star are significantly broadened by rotation ($v \sin i \approx 40$ km s^{-1}) and that we expect the $v \sin i$ of star 1 to be about the same, the spectral lines of the two stars are likely to be heavily blended at all phases, since the semiamplitude K_1 is of the same order as the combined rotational broadening. In cases such as this, traditional spectral analysis techniques are not very useful.

We re-examined our spectra using TODCOR (Zucker & Mazeh 1994), a two-dimensional cross-correlation technique that has the ability to use a different template for each star in a composite spectrum. With TODCOR it is often possible to measure accurate velocities for both stars even when the lines are severely blended. For the main star we used the same synthetic template as before (§ 2), and for star 1 we generated a synthetic spectrum based on the parameters predicted by the blend model: $T_{\rm eff} = 6750$ K, $\log g = 4.0$, $v \sin i = 40$ km s^{-1}, and an assumed solar metallicity. The correlation functions for the individual echelle orders were combined together in a manner analogous to the technique introduced by Zucker et al. (2003). Because of the similarity in temperature between the two stars (corresponding approximately to spectral types F4 and F6), the light ratio was assumed to be constant with wavelength.[12]

[12] Checks with low-resolution spectra of the appropriate temperatures indicate a change of only 10% in the flux ratio across the entire spectral window, a difference that is unimportant for our purposes.

As illustrated in Figure 8, the lines of star 1 are indeed clearly present in our spectra. The top panel shows a contour plot of the two-dimensional cross-correlation surface as a function of the velocities of star 1 and star 3. The maximum correlation is indicated by the dot and lies along a steep ridge line that runs vertically through the diagram, which is produced by the large difference in brightness between the two stars. Cuts through this surface at fixed values for the velocities of each star are indicated by the dashed lines and are shown in the lower two panels. The obvious peak in the lower panel is evidence that star 1 is clearly detected, and we were able to measure its velocity on all four of our spectra. The radial velocities we derive for both stars are given in Table 1. A spectroscopic orbital solution for star 1 from these velocities assuming a circular orbit and a fixed ephemeris from equation (1) gives a semiamplitude of 62 km s^{-1}, which is very close to the predicted value of 63 km s^{-1}. This orbit is shown in Figure 9. The spectroscopic light ratio (approximately in the visual band) measured with TODCOR is 0.15, also reasonably close to the prediction. The velocities for star 3, on the other hand, show much less variation than our original one-dimensional results from § 4 (see also Fig. 3). The rms residual from the mean is now 0.87 km s^{-1}, compared to 2.03 km s^{-1} for the velocities shown in Figure 3. This is an indication that the use of TODCOR has effectively removed the distortions (asymmetries) that initially suggested a velocity variation. We note also that the weighted average of the new velocities for star 3, -28.95 km s^{-1}, is very close to the center-of-mass velocity of the orbit for star 1, which is -29.34 km s^{-1}. This is just as expected for a physical triple system.

Given the uncertainties and assumptions in the blend model, the agreement in the properties of star 1 and the overall consistency of the results are quite remarkable, and it is entirely possible that an even closer agreement could be reached by

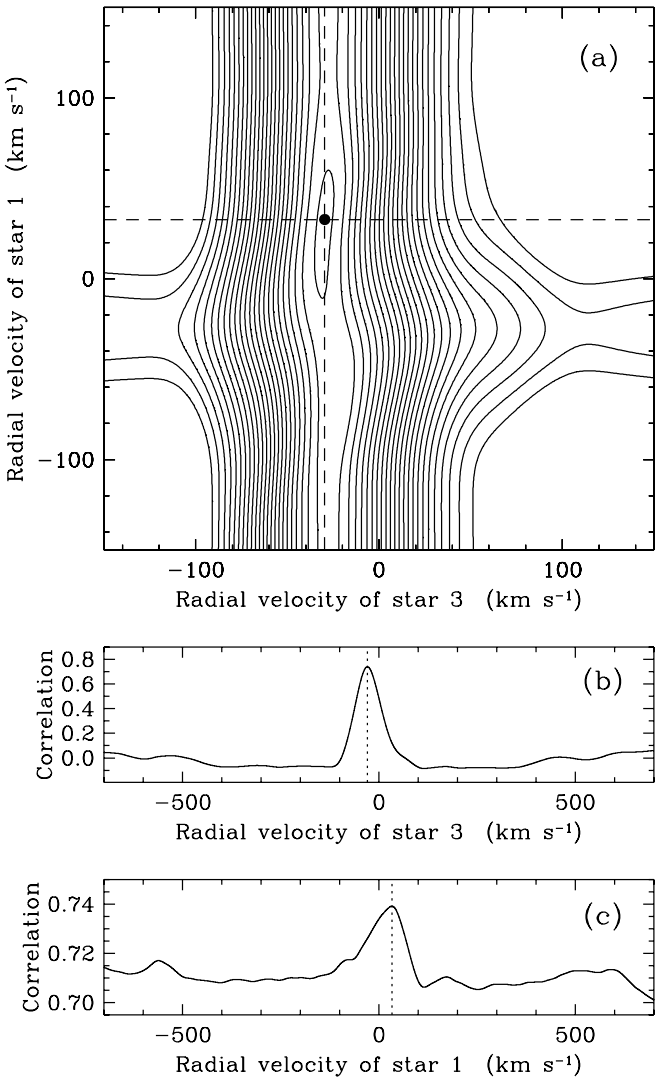

FIG. 8.—(*a*) Contour diagram of the two-dimensional cross-correlation surface computed with TODCOR for the last of our observations, as a function of the velocities of star 1 and star 3. The maximum is indicated by the dot, and the dashed lines represent cuts through the surface that are shown in the lower panels. (*b*) Cross section of the two-dimensional correlation function at a fixed velocity for star 1, showing the peak corresponding to the main star in OGLE-TR-33. The measured velocity is indicated by the dotted line. (*c*) Same as (*b*), but at a fixed velocity for star 3, showing the clear detection of star 1.

TABLE 1

RADIAL VELOCITY MEASUREMENTS FOR STAR 1 AND STAR 3 IN OGLE-TR-33

HJD (2,400,000+)	RV Star 1 (km s^{-1})	RV Star 3 (km s^{-1})
52480.8503.....	−89.12	−28.16
52481.9398.....	+32.92	−29.45
52482.9403.....	−91.24	−27.95
52483.9357.....	+32.78	−29.65

NOTE.—Velocities in the barycentric frame. Estimated errors are 1 and 0.5 km s^{-1} for star 1 and star 3, respectively, except for the first date (weak exposure), in which the uncertainties are twice as large.

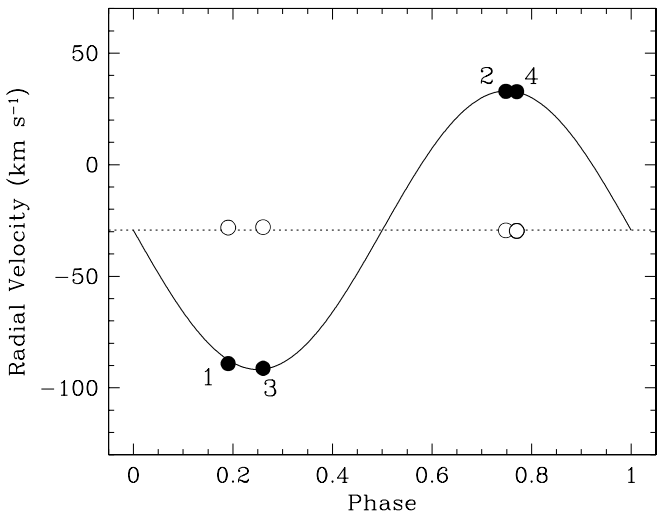

FIG. 9.—Radial velocities of star 1 (primary of the eclipsing binary blended with OGLE-TR-33) measured with TODCOR (*filled circles*). Dates are labeled as in Fig. 3*a*. Also shown is the corresponding spectroscopic orbital solution adopting the ephemeris from eq. (1), with the dotted line representing the center-of-mass velocity, γ. The velocities for star 3 are shown with open circles, and lie very close to γ. The error bars are smaller than the symbols.

fine-tuning various parameters of the model, although we have not considered this necessary here.

6. BLENDING ACROSS THE H-R DIAGRAM: A CAUTIONARY TALE

The example of OGLE-TR-33 presents a warning about the kinds of blend scenarios that may be the most challenging to expose. As we showed in § 5.2, the slightly evolved nature of the main star allows it to be significantly brighter intrinsically, and this in turn makes it easier to hide a fainter eclipsing binary in its glare that would typically be difficult to detect spectroscopically.

The situation is depicted more clearly in Figure 10, where we show evolutionary tracks for solar metallicity in a diagram of absolute visual magnitude as a function of effective temperature.[13] The heavy dashed lines indicate the zero-age main sequence (ZAMS) on the left and the red edge of the main sequence on the right, where stars have nearly exhausted their hydrogen fuel and are about to undergo the brief collapse phase that gives rise to the "blue hook" feature. The shaded area in between represents the full width of the main-sequence band. For most stars of spectral type G and later (spectral type boundaries are indicated along the bottom of the figure), the vertical extent of this region is only 0.5 mag or less. For hotter stars beginning at spectral type F, however, there is a significant widening of the main sequence such that the vertical extent can exceed 2 mag. It is precisely in this region of the H-R diagram that OGLE-TR-33 is located. Because stars here can evolve to be much brighter than unevolved stars of the same age, this leaves ample room for a fainter eclipsing binary along the same line of sight to go unnoticed. To make matters worse, F stars are typically very

[13] We have chosen for this illustration the models by Yi et al. (2003) over those of Girardi et al. (2000), used earlier, merely for their higher resolution near the turnoff.

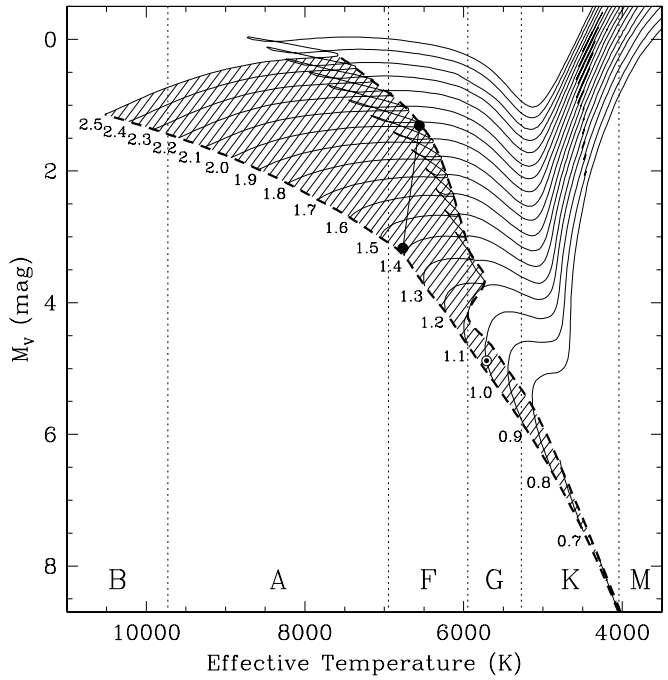

FIG. 10.—Evolutionary tracks from the series of models by Yi et al. (2003) for solar metallicity, with the mass of each track labeled on the left in solar masses. Thick dashed lines indicate the ZAMS (*left*) and the red edge of the main-sequence phase (*right*). The shaded area in between is where evolution makes stars intrinsically brighter (by up to 2 mag or more) while still on the main sequence, and leaves ample room for a fainter unevolved star to go undetected in the observations, producing a blend. We indicate the location of the Sun on the 1.0 $M_\odot$ track for reference, as well as the positions of star 1 and star 3 in OGLE-TR-33 (from Fig. 5) connected by a line. Approximate spectral type boundaries are indicated along the bottom.

common in magnitude-limited samples such as OGLE-III, for the very same reason that they are brighter.

In blend cases in which star 1 and star 3 have very different effective temperatures (and colors), photometric follow-up in multiple passbands can be an efficient way to discover the false positive, since the transit depth will depend on wavelength (see, e.g., Kotredes et al. 2004). However, blends composed of stars of similar temperature will *not* show a significant color dependence, and once again OGLE-TR-33 is one such example. On the basis of the above, we predict that blends with no significant color dependence to the eclipse depth may be more common than previously thought among F stars. Therefore, special care is required when investigating F stars with transit signatures, since the signs of the eclipsing binary may not be immediately obvious in either the photometry or the spectroscopy.

7. CONCLUDING REMARKS

Transit searches for extrasolar planets have attracted a great deal of attention in recent years, driven by the excitement following the discovery of HD 209458 and more recently OGLE-TR-56, OGLE-TR-113, and OGLE-TR-132 (Konacki et al. 2003a, 2004; Bouchy et al. 2004). Since no other examples as bright as HD 209458 ($V = 7.65$) have been found to date, focus has quickly shifted to denser fields and fainter stars. As researchers involved in these searches have learned by now, candidates are relatively easy to find, but the large number of astrophysical false positives is a very serious issue, particularly for these fainter targets. Blending is perhaps the most insidious of these effects, and is likely to be exacerbated in F stars because of the widening of the main sequence. The problem of finding true transiting planets around faint stars has essentially become one of ruling out the possibility that a given candidate can be anything else ("discovery by elimination"). Similar or perhaps more challenging difficulties will be faced by future space projects designed to search for even smaller planets, such as NASA's *Kepler* mission.

In the preceding sections, we have shown that the complete set of observations available for the transiting planet candidate OGLE-TR-33 can in fact be adequately explained as being the result of a fairly typical blend scenario, and therefore that the photometric signature that originally drew attention to it is very unlikely to be due to a planet crossing in front of the star. In this case the configuration is a hierarchical triple system with an age of $\sim$1 Gyr composed of an eclipsing binary (F4 V + K7–M0 V) and a slightly evolved and brighter F6 star that dilutes the light of the close pair. The self-consistent model we have constructed is able to account for all photometric and spectroscopic constraints, including the detailed morphology of the light curve (depth, duration, and shape), as well as the composite nature of the spectrum, the velocity amplitude of star 1, and its brightness relative to the main star.

Achieving this level of agreement is of course not normally the goal of follow-up observations of transit candidates. Rather, our motivation here has been to show how a detailed modeling of the light curve can provide important clues as to what other effects to look for in the data that might produce compelling evidence against the planet hypothesis.

The scenario found to reproduce the observations for this particular candidate is but one in an enormous variety of possible configurations involving an eclipsing binary and another star. Other such examples have been reported recently, e.g., by Charbonneau et al. (2004) from another search program. OGLE-TR-33 is especially interesting in that it serves to highlight how subtle the signs of a blend can be: in this case, the relatively small variations in the profiles of the spectral lines. Had these variations been smaller (or our spectroscopic observations of lower quality), they might have been overlooked. The importance of careful follow-up cannot be overstated, and alternate explanations should always be examined. If a candidate with transit-like events of the right characteristics (shape, depth, and duration) shows no other evidence of contamination from an eclipsing binary (spectroscopic or otherwise), can it *still* be a blend? This possibility must be thoroughly explored before a claim can be made with any confidence. Qualitative arguments or "back-of-the-envelope" calculations are generally insufficient, and we believe that analytical tools such as the one we have developed and applied in this paper can be extremely helpful to guide the investigation. In a forthcoming paper we will explore quantitatively the effects of blend scenarios on spectral line asymmetries and radial velocities measured by cross-correlation.

We are grateful to A. Udalski and the OGLE team for numerous contributions to this project, and to the referee for helpful comments. Some of the data presented herein were obtained at the W. M. Keck Observatory, which is operated as a scientific partnership among the California Institute of Technology, the University of California, and the National Aeronautics and Space Administration. The Observatory was made

possible by the generous financial support of the W. M. Keck Foundation. G. T. acknowledges support for this work from NASA's *Kepler* mission, STScI program GO-9805.02-A, the Keck PI Data Analysis Fund (JPL 1257943), and NASA Origins grant NNG04LG89G. M. K. gratefully acknowledges the support of NASA through the Michelson fellowship program. S. J. thanks the Miller Institute for Basic Research in Science at UC Berkeley for support through a research fellowship. This research has made use of NASA's Astrophysics Data System Abstract Service.

REFERENCES

Barlow, T. 2002, MAKEE Keck Observatory HIRES Data Reduction Software (Pasadena: Caltech), http://spider.ipac.caltech.edu/staff/tab/makee
Bouchy, F., Pont, F., Santos, N. C., Melo, C., Mayor, M., Queloz, D., & Udry, S. 2004, A&A, 421, L13
Brown, T. 2003, ApJ, 593, L125
Butler, R. P., Marcy, G. W., Vogt, S. S., Fischer, D. A., Henry, G. W., Laughlin, G., & Wright, J. T. 2003, ApJ, 582, 455
Cardelli, J. A., Clayton, G. C., & Mathis, J. S. 1989, ApJ, 345, 245
Charbonneau, D., Brown, T. M., Dunham, E. W., Latham, D. W., Looper, D. L., & Mandushev, G. 2004, in AIP Conf. Proc. 713, The Search for Other Worlds, ed. S. S. Holt & D. Deming (New York: Springer), 151
Charbonneau, D., Brown, T. M., Latham, D. W., & Mayor, M. 2000, ApJ, 529, L45
Charbonneau, D., Brown, T. M., Noyes, R. W., & Gilliland, R. L. 2002, ApJ, 568, 377
Claret, A. 2000, A&A, 363, 1081
Cox, A. N. 2000, Allen's Astrophysical Quantities (4th ed.; New York: Springer), 389
Drake, A. J. 2003, ApJ, 589, 1020
Duquennoy, A., & Mayor, M. 1991, A&A, 248, 485
Etzel, P. B. 1981, in Photometric and Spectroscopic Binary Systems, ed. E. B. Carling & Z. Kopal (Dordrecht: Reidel), 111
Girardi, L., Bressan, A., Bertelli, G., & Chiosi, C. 2000, A&AS, 141, 371
Gray, D. F. 1992, The Observation and Analysis of Stellar Photospheres (2nd ed.; Cambridge: Cambridge Univ. Press), 417
Henry, G. W., Marcy, G. W., Butler, R. P., & Vogt, S. S. 2000, ApJ, 529, L41
Horne, K. 2003, in ASP Conf. Ser. 294, Scientific Frontiers of Research on Extrasolar Planets, ed. D. Deming & S. Seager (San Francisco: ASP), 361
Hut, P. 1981, A&A, 99, 126
Kallrath, J., & Milone, E. F. 1999, Eclipsing Binary Stars: Modeling and Analysis (New York: Springer), 196
Konacki, M., Torres, G., Jha, S., & Sasselov, D. D. 2003a, Nature, 421, 507
Konacki, M., Torres, G., Sasselov, D. D., & Jha, S. 2003b, ApJ, 597, 1076
Konacki, M., et al. 2004, ApJ, 609, L37
Kotredes, L., Charbonneau, D., Looper, D. L., & O'Donovan, F. T. 2004, in AIP Conf. Proc. 713, The Search for Other Worlds, ed. S. S. Holt & D. Deming (New York: Springer), 173
Kurtz, M. J., & Mink, D. J. 1998, PASP, 110, 934
Kurucz, R. L. 1993, ATLAS9 Stellar Atmosphere Programs and 2 km s^{-1} Grid, Kurucz CD-ROM No. 13 (Cambridge: SAO)
Latham, D. W. 2003, in ASP Conf. Ser. 294, Scientific Frontiers in Research on Extrasolar Planets, ed. D. Deming & S. Seager (San Francisco: ASP), 409
Mallén-Ornelas, G., Seager, S., Yee, H. K. C., Minniti, D., Gladders, M. D., Mallén-Fullerton, G. M., & Brown, T. M. 2003, ApJ, 582, 1123
Mandel, K., & Agol, E. 2002, ApJ, 580, L171
Mazeh, T., et al. 2000, ApJ, 532, L55
Metcalfe, T. S., Mathieu, R. D., Latham, D. W., & Torres, G. 1996, ApJ, 456, 356
Naef, D., Mayor, M., Beuzit, J. L., Perrier, C., Queloz, D., Sivan, J. P., & Udry, S. 2004, A&A, 414, 351
Nelson, B., & Davis, W. 1972, ApJ, 174, 617
Oppenheimer, B. R., Kulkarni, S. R., & Stauffer, J. R. 2000, in Protostars and Planets IV, ed. V. Mannings, A. P. Boss, & S. S. Russell (Tucson: Univ. of Arizona Press), 1313
Popper, D. M., & Etzel, P. B. 1981, AJ, 86, 102
Queloz, D., et al. 2001, A&A, 379, 279
Ribas, I. 2003, A&A, 398, 239
Sabbey, C. N., et al. 1995, ApJ, 446, 250
Santos, N. C., et al. 2002, A&A, 392, 215
Schneider, J. 2004, The Extrasolar Planet Encyclopaedia (Paris: Obs. Paris), http://www.obspm.fr/encycl/encycl.html
Seager, S., & Mallén-Ornelas, G. 2003, ApJ, 585, 1038
Sirko, E., & Paczyński, B. 2003, ApJ, 592, 1217
Tingley, B. 2004, A&A, in press (astro-ph/0406201)
Tinney, C. G., Butler, R. P., Marcy, G. W., Jones, H. R. A., Penny, A. J., Vogt, S. S., Apps, K., & Henry, G. W. 2001, ApJ, 551, 507
Tokovinin, A. A. 1997, Astron. Lett., 23, 727
Tokovinin, A. A., & Smekhov, M. G. 2002, A&A, 382, 118
Torres, G., Konacki, M., Sasselov, D. D., & Jha, S. 2004, ApJ, 609, 1071
Torres, G., & Ribas, I. 2002, ApJ, 567, 1140
Udalski, A. 2003, ApJ, 590, 284
Udalski, A., Pietrzyński, G., Szymański, M., Kubiak, M., Żebruń, K., Soszyński, I., Szewczyk, O., & Wyrzykowski, Ł. 2003, Acta Astron., 53, 133
Udalski, A., Szewczyk, O., Żebruń, K., Pietrzyński, G., Szymański, M., Kubiak, M., Soszyński, I., & Wyrzykowski, Ł. 2002a, Acta Astron., 52, 317
Udalski, A., Szymański, M., Kałuzny, J., Kubiak, M., & Mateo, M. 1992, Acta Astron., 42, 253
Udalski, A., Żebruń, K., Szymański, M., Kubiak, M., Soszyński, I., Szewczyk, O., Wyrzykowski, Ł., & Pietrzyński, G. 2002b, Acta Astron., 52, 115
Udalski, A., et al. 2002c, Acta Astron., 52, 1
Vidal-Madjar, A., Lecavelier des Etangs, A., Désert, J.-M., Ballester, G. E., Ferlet, R., Hébrard, G., & Mayor, M. 2003, Nature, 422, 143
Vidal-Madjar, A., et al. 2004, ApJ, 604, L69
Vogt, S. S., et al. 1994, Proc. SPIE, 2198, 362
Yee, H. K. C., Mallén-Ornelas, G., Seager, S., Gladders, M. D., Brown, T., Minniti, D., Ellison, S., & Mallén-Fullerton, G. 2003, Proc. SPIE, 4834, 150
Yi, S. K., Kim, Y., & Demarque, P. 2003, ApJS, 144, 259
Zucker, S., & Mazeh, T. 1994, ApJ, 420, 806
Zucker, S., Mazeh, T., Santos, N. C., Udry, S., & Mayor, M. 2003, A&A, 404, 775